Numerical Simulation of a Solar Flat Plate Collector using Discrete Transfer Radiation Model (DTRM) – A CFD Approach

K. Vasudeva Karanth [1*]   Manjunath M. S.[2]   N. Yagnesh Sharma[3], *Member, IAENG*

Abstract— **Solar flat plate collectors are commonly used for domestic and industrial purposes and have the largest commercial application amongst the various solar collectors. This is mainly due to simple design as well as low maintenance cost. An attempt is being made in this paper to numerically analyze the solar collector using the Discrete Transfer Radiation Model (DTRM) so as to numerically simulate the solar collector for better understanding of the heat transfer capabilities of the collector. In the present work a 3D model of the collector involving the water pipe, absorber plate, the glass top and the air gap in-between the absorber plate and the glass top is modeled to provide for conduction, convection and radiation in the analysis. The numerical results obtained using Computational fluid dynamics (CFD) by employing conjugate heat transfer show that the heat transfer simulation due to solar irradiation to the fluid medium, increases with an increase in the mass flow rate. Also it is observed that the absorber plate temperature decreases with increase in the mass flow rate.**

Index Terms—**Conjugate heat transfer, Solar irradiation simulation, Solar collector, Discrete transfer radiation model, Solar load model.**

I. INTRODUCTION

Solar energy collectors are special kind of heat exchangers that transform solar radiation energy to internal energy of the transport medium. The major component of any solar system is the solar collector. Of all the solar thermal collectors, the flat plate collectors though produce lower temperatures, have the advantage of being simpler in design, having lower maintenance and lower cost.

There is a host of literature on glazed solar collectors. Sopian et al. [2] experimentally studied the performance of a new design of non-metallic unglazed solar water heater integrated with a storage system. An analysis based upon the

[1] Corresponding Author: Associate Professor, Dept of Mechanical and Manufacturing Engg, Manipal Institute of Technology, Manipal University, Manipal, Karnataka State, India. kvkaranth@gmail.com
[2] Research Scholar Dept of Mechanical and Manufacturing Engg, Manipal Institute of Technology, Manipal University, Manipal, Karnataka State, India. manjunathNITC@gmail.com
[3], Professor, Dept of Mechanical and Manufacturing Engg, Manipal Institute of Technology, Manipal University, Manipal, Karnataka state, India. nysharma@hotmail.com, Ph: +91-9480485082.

two-dimensional finite element method to characterize the performance of solar collectors was done by Gorla [3]. Turgut et. al. [4] conducted an experimental and three dimensional numerical work to determine the average heat transfer coefficients for forced convection air flow over a rectangular flat plate. Selmi et al. [5] performed a CFD simulation of flat plate solar energy collector with water flow. The CFD model was validated with experimental results. Janjai et al. [6] developed a mathematical model for simulating the performance of a large area plastic solar Collector. Lecoeuche and Lalot [7] applied neural network technique to predict the thermal performance of a solar flat plate collector.

Jorge and Armando [8] conducted a numerical study on a new trapezoidal cavity receiver for a linear Fresnel solar collector using DTRM Model. The main assumption is that the radiation leaving the surface element in a certain range of solid angle can be approximated by a single ray. Luis Candanedo et al. [9] developed convective heat transfer coefficients for several different Building–Integrated Photovotaic/ thermal systems using CFD. They used DTRM model and the fluid was modeled as Non-participating media for radiation exchange.

It is found from the literature that the CFD simulation of the solar flat plate collector using the DTRM model is not available and hence a numerical simulation using CFD technique is carried out in this study.

II. NOMENCLATURE

T   Temperature
C_T Temperature rise coefficient
x   Distance along the absorber plate
L   Length of the collector
C_L Non-dimensional collector length (x/L)
U   Velocity
ρ Density
μ Viscosity
P_r Prandtl Number

Suffix; 1 – inlet, 2 - outlet

III. NUMERICAL FORMULATIONS

A. *Problem statement and assumptions*

The flow domain consists of an absorber plate of 1 m length, 150 mm wide and 2 mm in thickness. A circular absorber tube is attached below the absorber plate and the pipe is 10 mm in diameter with a thickness of 1 mm. The absorber plate is covered with a glass plate of 5 mm thickness with an air gap of 5 mm. The configuration is as shown in figure 1. The water tube is placed centrally and the water enters the tube from its back end. The following assumptions are made in the analysis.

(1) Water is a continuous medium and incompressible.
(2) The flow is steady and possesses laminar flow characteristics, as the velocity of flow is low.
(3) The thermal-physical properties of the absorber plate and the absorber tube are constant with respect to the operating temperature.
(4) The bottom side of the absorber tube and the absorber plate is assumed to be adiabatic.
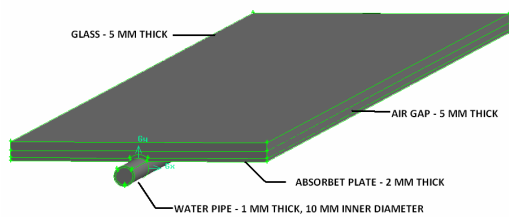
Fig.1 Geometry of the flat plate collector

B. Numerical model

Numerical simulation is carried out with steady state implicit pressure based solver using the Fluent 6.3 code. The governing partial differential equations, for mass and momentum are solved for the steady state flows. The pressure-velocity coupling is carried out using the SIMPLE algorithm [1]. Discretization is done using the second order upwind scheme. Discrete Transfer Radiation Model (DTRM) is adopted for the radiation heat transfer and the solar insolation is input using solar load model inbuilt in the Fluent code[10].The solar calculator is used to track the solar irradiation for the analysis by taking 21st February as the day for the sun shine with fair weather conditions in the region where the experimentation was carried out. A longitude and latitude angle of 74.79347^{0} and 13.35077^{0} which correspond to the region where the model is experimented is found from the Google earth to calculate the solar radiation. The analysis is carried out for 11 am, 12 noon and 1 pm of the day using the above procedure.

C. Mean Flow Equations

All the equations are presented in Cartesian tensor notation.

Continuity:

$$\frac{\partial}{\partial x_i}(rU_i) = 0 \qquad (1)$$

Momentum equation

$$\frac{\partial}{\partial x_j}(rU_iU_j) = \frac{\partial P}{\partial x_i} + \frac{\partial}{\partial x_j}\left[m\left(\frac{\partial U_i}{\partial x_j} + \frac{\partial U_j}{\partial x_i}\right) - r\overline{u_iu_j}\right] \qquad (2)$$

Energy equation

$$\frac{\partial}{\partial x_j}(rU_iT) = \frac{\partial}{\partial x_j}\left[\frac{m}{\mathrm{Pr}}\frac{\partial T}{\partial x_j} - r\overline{u_it}\right] \qquad (3)$$

IV. METHOD OF SOLUTION

A. Numerical scheme

The three dimensional computational domain is modeled using hex mesh as shown in Figure 2. The complete domain consists of 1.6 million elements which include the water, water tube absorber plate, air and glass medium.

The grid independence test was performed to check validity of the quality of mesh on the solution. The influence of further refinement did not change the result by more than 1.25 % which is taken here as the appropriate mesh quality for computation.
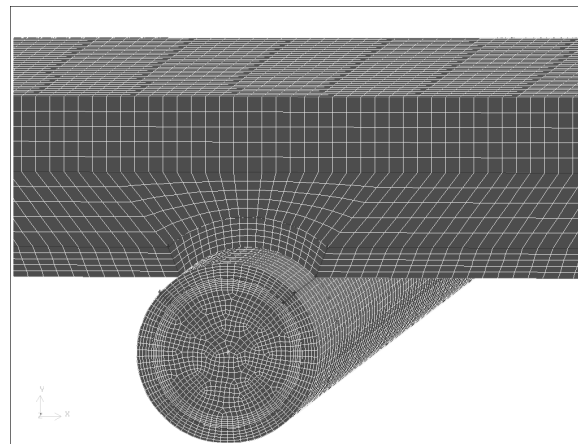
Fig.2 Localized view of the meshed computational domain

Conservation equations were solved for the control volume to yield the velocity and temperature fields for the water flow in the absorber tube and the temperature fields for the absorber plate. Convergence was effected when all the residuals fell below 1.0e-6 in the computational domain.

B. Boundary Conditions and Operating Parameters

Appropriate boundary conditions were impressed on the computational domain, as per the physics of the problem.

For the inlet a 'velocity inlet' boundary condition is specified and an 'outflow' condition is specified at the outlet for the water continuum. The glass top surface is exposed to solar irradiation. The glass material is made up of Borosilicate which has a thermal conductivity of 1.14 W/mK and a refractive index of 1.47. The specific heat is taken as 750 J/kg-K. The absorber plate and the absorber tube is made up of copper material.

Wall boundary conditions were used to bound fluid and solid regions. In viscous flow models, at the wall, velocity

components were set to zero in accordance with the no-slip and impermeability conditions that exist there.

The interface between the water and the absorber tube is defined as wall with coupled condition to effect conjugate heat transfer from absorber tube to the water.

The analysis is carried out for three different time conditions i.e. 11 am, 12 noon and 1 pm of the day and six different inlet conditions which are Velocity V1= 0.0001 m/s, V2 = 0.0005 m/s, V3 = 0.001 m/s, V4 = 0.005 m/s, V5 = 0.01m/s and V6 = 0.05 m/s.

The Temperature coefficient C_T is calculated using eq. (4)

$$C_T = \frac{T - T_1}{T_2 - T_1} \qquad (4)$$

V. RESULTS AND DISCUSSION

The simulation is carried out at 3 different times of the day and the results are shown in figures 3 to 16. From figures 3 and 4, it is clearly seen that the absorber plate gets almost uniformly heated corresponding to various velocities. Whereas the water in the absorber tube gets differentially heated with very high temperature rise for lower mass flow rate followed by almost constant heat transfer at the same temperature. In figure 3 corresponding to different flow rates the absorber plate temperature initially has higher temperature vis-à-vis lower velocities of flow. This is due to the fact that at lower velocities, the convective component of the flowing water in the absorber tube is very limited and hence heat dissipation from the absorber plate to the water is not significant. However with increased velocity of flow, convective effect brings down the absorber plate temperature as shown in figure 3.

In a similar manner with the increasing velocity of flow, the water temperature of the fluid decreases with increase in flow velocity. The tendency of flowing water in the absorber tube to absorb heat gets reduced due to better mixing at higher velocities corresponding to the higher mass flow rate. It is discernable from the figures 5 to 7 that the temperature profiles almost nearly remain constant after initial transient rise. This may be due to extremely small velocity employed in the simulation so as to correspond to natural buoyancy driven flow in real life situations.

A non-dimensional temperature rise coefficient (C_T) is plotted against non-dimensional flow length along the computational domain as shown in figures 5 to 10. It is interesting to note that whereas for smaller velocities, the gradient of temperature profiles for the absorber plate rapidly increases, the temperature gradient for the water in the absorber tube show a lower temperature gradient. This can be explained from the fact that the absorber plate gets cooled faster with increase in mass flow rate thus producing steep temperature gradient. Contrastingly, the temperature gradient of profile for water decreases with increase in mass flow rate due to better convective capability of the medium at higher velocities. It is also observed from figures 5 to 10 that the temperature difference band between the absorber plate and the water increases as the flow rate increases, due to higher thermal resistance between absorber plate and

flowing water. The numerical simulation is carried out in a similar manner corresponding to the other times of the day i.e. 12 noon and 11 am as shown in figures 11 to 15. It is found from figures 3, 11 and 13 that as the sun moves in the horizon from east to west between 11 am to 1 pm, the intensity of solar irradiation increases and then decreases due to peak intensity at 12 noon. This is reflected in the absorber plate temperature plots with an increase in temperature corresponding to 12 noon as in figure 11 compared to lower levels of heating as seen from figure 3 and 13.
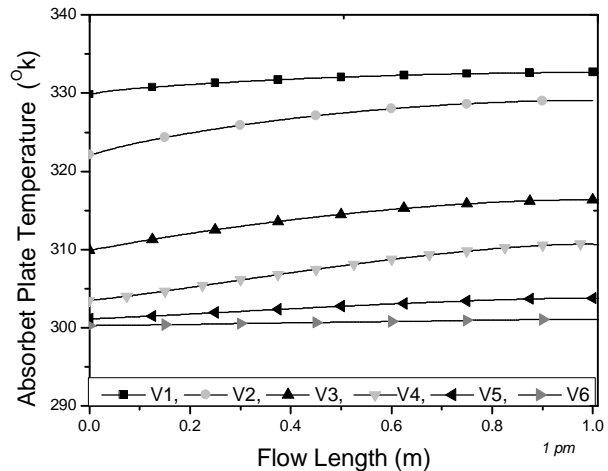
Fig. 3. Absorber plate temperature plot corresponding to 1 pm vs varying velocity of water
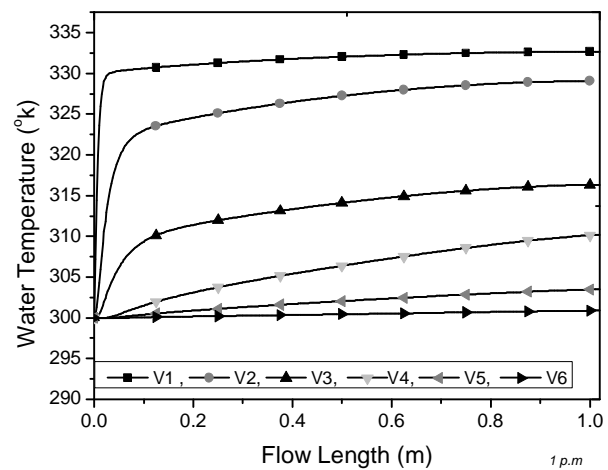
Fig. 4. Water temperature plot corresponding to 1 pm vs. varying velocity of water
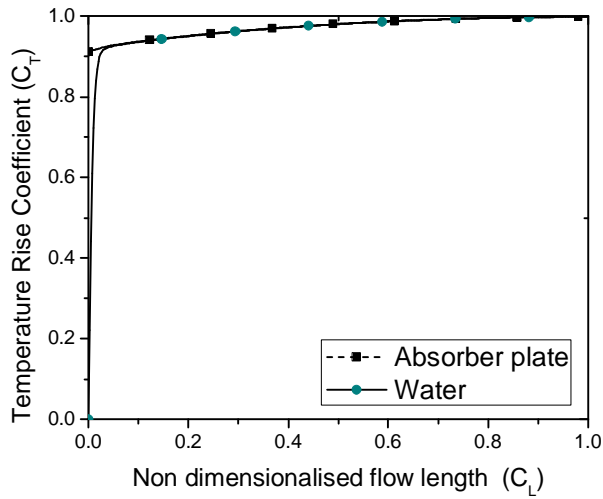
Fig 5. Temperature rise coefficient of absorber plate and water at 1 pm corresponding to flow velocity V_1.
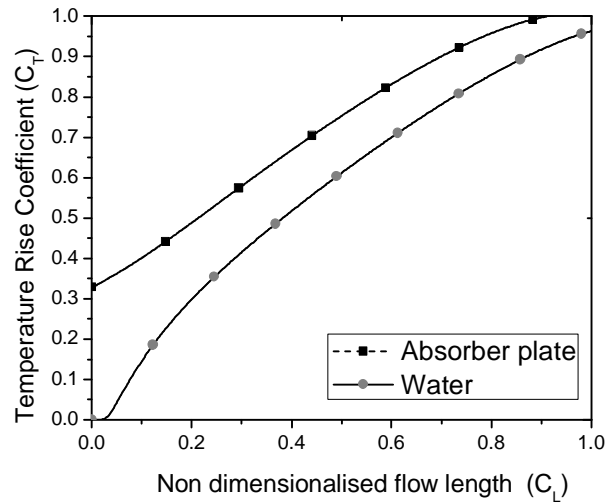
Fig 8. Temperature rise coefficient of absorber plate and water at 1 pm corresponding to flow velocity V_4.
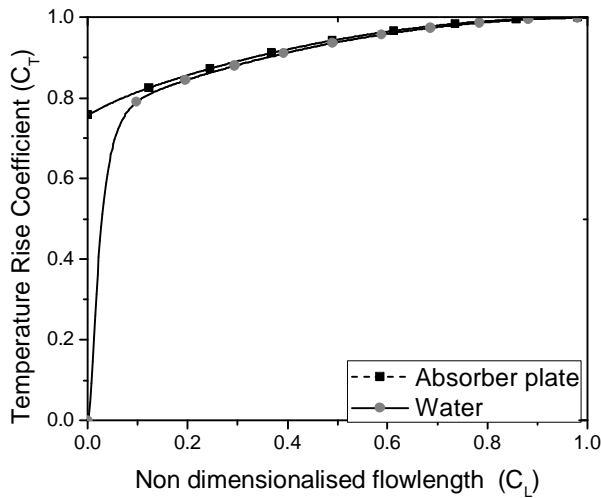
Fig 6. Temperature rise coefficient of absorber plate and water at 1 pm corresponding to flow velocity V_2.
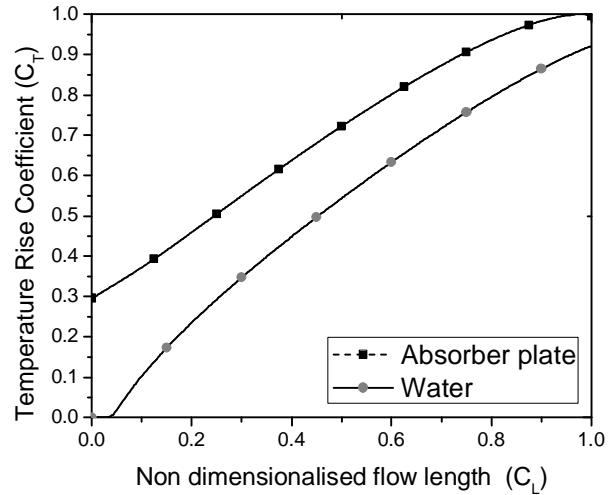
Fig 9. Temperature rise coefficient of absorber plate and water at 1 pm corresponding to flow velocity V_5.
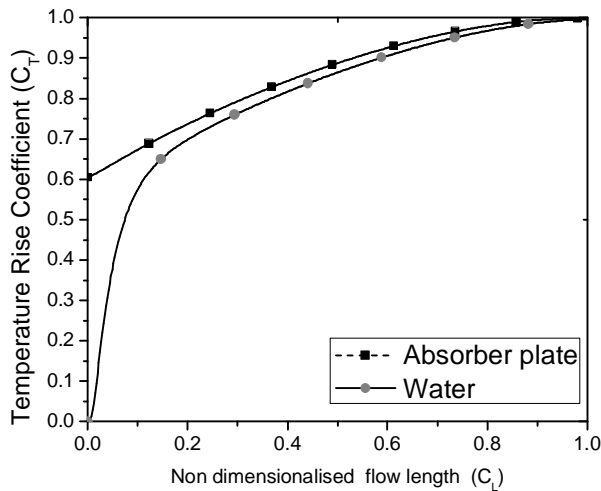
Fig 7. Temperature rise coefficient of absorber plate and water at 1 pm corresponding to flow velocity V_3.
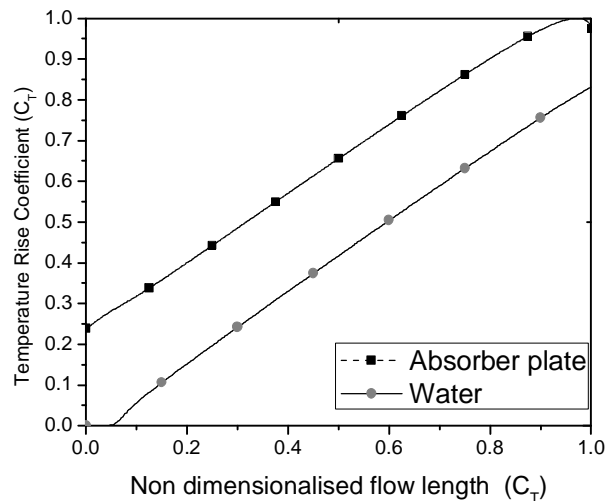
Fig 10 Temperature rise coefficient of absorber plate and water at 1 pm corresponding to flow velocity V_6.
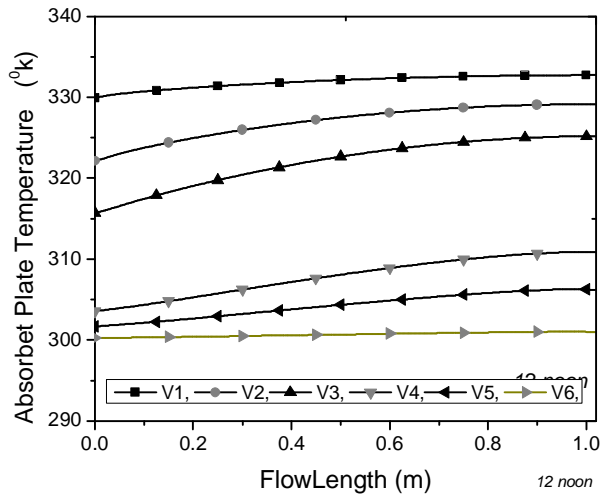
Fig. 11 Absorber plate temperature plot corresponding to
12 noon vs. varying velocity of water
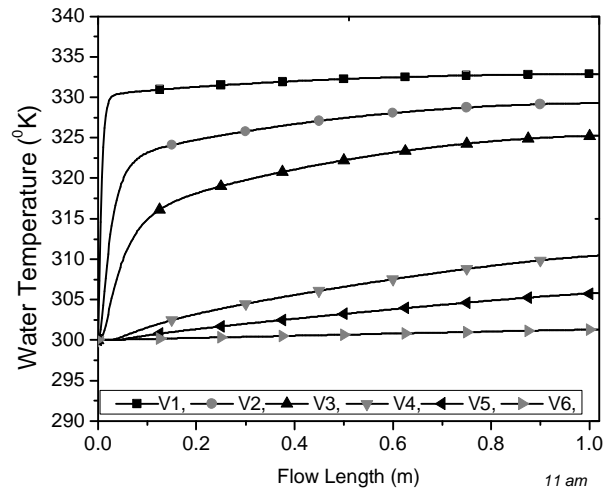
Fig. 12 Water temperature plot corresponding to 12 noon vs. varying
velocity of water

Fig. 13 Absorber plate temperature plot corresponding to
11 am vs. varying velocity of water

Fig. 14 Water temperature plot corresponding to 11 am vs. varying velocity
of water
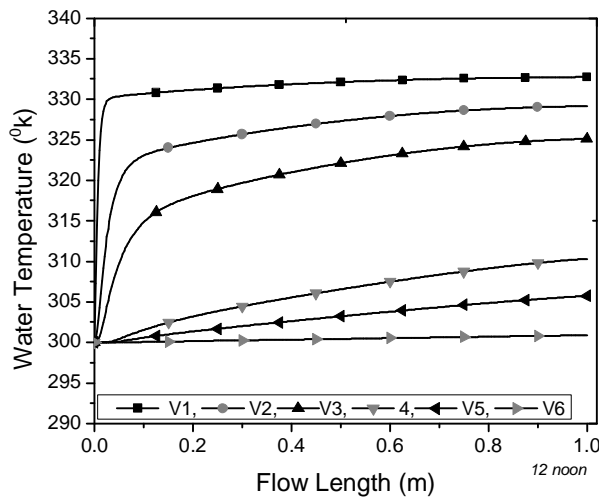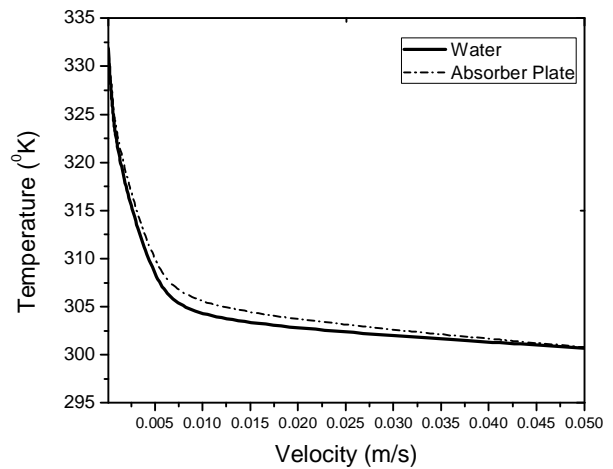
Fig 15. Average temperature plot of absorber plate and water vs. varying
mass flow rate corresponding to 1 pm
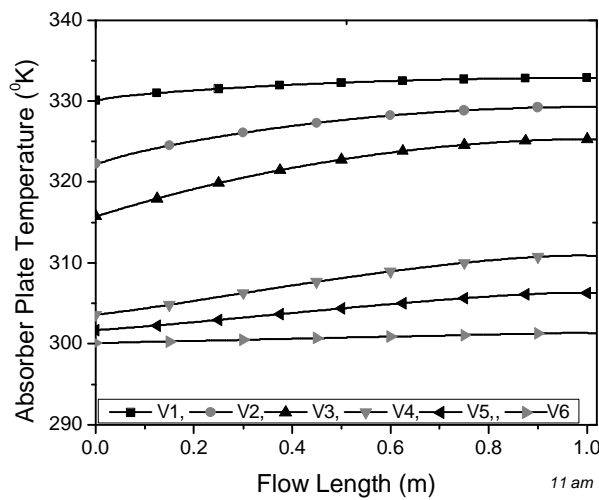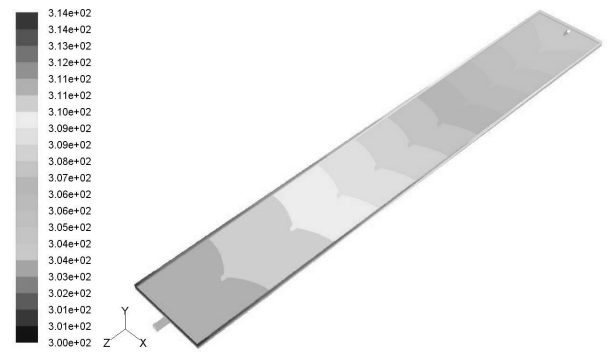
Fig 16 3D Temperature contour plot of absorber plate corresponding to 1
pm at flow velocity v4.

Figure 15 shows the average temperature plot for both
absorber plate and the water corresponding to 1 pm and with
varying mass flow rate. It can be noted that the temperature
drop due to convection between the two media is steeper at
lower mass flow rate than at higher mass flow rate. Figure
16 shows the temperature contour plot of one of the models
at medium mass flow rate.

CONCLUSION

The following conclusions are deduced from the above numerical simulation:

- Absorber plate temperature is almost linear at all the flow velocities considered.
- The water in the absorber tube suffers a steep temperature gradient initially followed by a near constant linear variation.
- Temperature rise coefficient shows contrasting trend with the absorber plate and water in the absorber tube.
- It is found from the analysis that the temperature differential between absorber plate and fluid keeps increasing with increase in flow velocity.
- Corresponding to different times of the day chosen in the analysis, the trend lines show similar attributes for varying mass flow rate.

REFERENCES

[1] Patankar S. V. and Spalding, D. B. "A calculation procedure for heat, mass and momentum transfer in three-dimensional parabolic flows", International Journal of Heat Mass Transfer, 1972, vol. 15, p. 1787.

[2] K. Sopian, M. Syahri, S. Abdullah, M. Y. Othman, B. Yatim, "Performance of a non-metallic unglazed solar water heater with integrated storage system", *Renewable Energy*, vol. 29, 2004, pp. 1421–1430.

[3] Gorla, R. S. R, "Finite element analysis of a flat plate solar collector", *Finite Elements in Analysis and Design*, vol.24, 1997, pp. 283-290.

[4] Turgut, O. and Onur, N, "Three dimensional numerical and experimental study of forced convection heat transfer on solar collector surface", *International Communications in Heat and Mass Transfer*, vol. 36, 2009, pp. 274-279.

[5] Selmi, M., Al-Khawaja, M. J., and Marafia, A., "Validation of CFD simulation for flat plate solar energy collector", *Renewable Energy*, vol.33, 2008, pp. 383-387.

[6] Janjai, S., Esper, A., Muhlbauer, W., "Modelling the performance of a large area plastic solar collector", Renewable energy, vol. 21, 2000, pp. 363-376.

[7] Lecoeuche, S. and Lalot, T. S., "Prediction of the daily performance of solar collectors", *International Communications in Heat and Mass Transfer,* vol.32, 2005, pp. 603–611.

[8] Jorge, F. and Armando O., "Numerical simulation of a trapezoidal cavity receiver for a linear Fresnel solar collector concentrator", *Journal of Renewable Emergy*, vol. 36, 2011, pp. 90 – 96.

[9] Candanedo, L., William O'Brien and Andrieas A., "Development of an air based open loop building –Integrated Photo votaic / thermal system model", *Proc. of 11th Int. IBPSA Conference*, July 27 – 30, 2009, Glasgow, Scotland.

[10] Fluent 6.3, Fluent Inc., Cavendish Court Lebanon, NH, 03766, USA.

[11] User's guide, Volume I to IV.